

Time dependence of morphology and mechanical properties of injection moulded recycled poly(ethylene-terephthalate)

Béla Molnár, Ferenc Ronkay*

Department of Polymer Engineering, Faculty of Mechanical Engineering, Budapest

University of Technology and Economics,

H-1111 Budapest, Műegyetem rkp. 3, Hungary

* Corresponding author. Tel.: +36 1 463-2462.

E-mail address: ronkay@pt.bme.hu (F. Ronkay).

Abstract

During research, injection moulded samples were prepared from recycled poly(ethylene-terephthalate) granulate, and their mechanical properties were investigated as a function of time. To understand the changes in mechanical properties, both morphology of injection moulded samples and recycled granulates were investigated. A three-phase morphological model was applied for the evaluation of morphological properties while mechanical properties were determined by tensile and impact tests. Relationship was found between morphological and mechanical characteristics as a function of time elapsed since production. Crystalline ratio, tensile strength, and modulus of injection moulded specimens increased while impact strength decreased in the four weeks after production.

1. Introduction

Nowadays PET is classified as commercial plastic. Its main application area is packaging (of mineral water and soft drinks) besides fiber production. Most products are used only once, hence have a short life cycle. Due to increasing usage and by stricter environmental regulations recycled PET (RPET) is a secondary raw material available in large amount. Its main application field is textile industry, while usage as packaging material either purely or as a

component of a mixture is also more and more significant. RPET is also present in other fields (such as sheets, technical parts) only in small amounts (Welle, 2011). Different blends of recycled PET, such as PET/HDPE (Dobrowszky and Ronkay, 2015), PET/PP (Tao et al., 2007), and their composites (Lei et al., 2009) are popular research topics due to other polymers found in the waste. Several investigations were carried out also on its applicability as matrix material in nanocomposites (Meri et al., 2014; Zare, 2013). RPET application possibilities are also researched in the construction industry in more fields: as additive in asphalt (Moghaddam et al., 2015), in concrete (Choi et al., 2009) and in mortar (Ge et al., 2014) since it modifies not only mechanical properties but also density, and as a base material in flame retardant facing/insulation elements. Application as base material of injection moulded products has serious significance in the future since it is one of the most frequently used polymer processing technologies. Several investigations have been carried out in this field (Torres et al., 2000; López et al., 2014) but there are still less known and less explained phenomena and based on their deeper understanding application areas of recycled PET can be extended.

Considering processing of recycled PET and the properties of products made of it the largest problem is small molecular weight, partly due to the molecular weight of the initial material (bottle grindings) and partly due to the effect of degradation during processing (Paci and Mantia, 1999; Assadi et al., 2004). The material can be subject to serious degradation in recycling processes due to heat, shearing and its moisture content. Due to the decrease in molecular weight the impact strength (toughness) of the product can decrease dramatically and that limits applicability to a great extent (Badia et al., 2012).

In case of recycled PET applied as a secondary base material it is essential to improve mechanical (strength, impact strength) and other properties (such as flame resistance, gas tightness) that influence its usage. As a result, new application areas are revealed (injection moulded interior parts for automotive applications, such as car-door handle or covers, mass-

produced goods, such as food or storage containers) besides the already existing ones. Degradation during re-processing can be compensated with chain extension additives that create chemical bonds among the molecular chains of molten PET and therefore increase molecular length (Incarnato et al., 2000; Karayannidis et al., 2000; Raffa et al., 2012). Since crystallization rate of PET is low, large cycle time is necessary for crystalline structure to be formed during injection moulding. If nucleating agents are applied more crystalline nuclei are formed in the material, therefore crystallization takes place more quickly, a more even, finer crystalline structure is formed in the product and therefore mechanical properties may improve (Hao et al., 2012). Similarly to other polymers, application of PET as reinforcing material in composites is also widespread because with its application significant property changes can be achieved. The strength and modulus of the base material can be improved significantly with different fiber reinforcements (such as glass, carbon or natural fibers) (Pegoretti and Penati, 2004).

In case of recycled PET processing morphological structure formed in the product is essential since it determines the mechanical properties. This structure can be examined by using several methods (Hsiao et al., 2013), the most significant among which are optical (Viana et al., 2004) and electron microscopy (Badia et al., 2012), differential scanning calorimetry (DSC) (Hamonic et al., 2014), X-ray diffraction (Alvarez et al., 2004; Gowd et al., 2004) and infrared examination (Karagiannidis et al., 2008). Recently PET is investigated by using a three-phase morphological model, in which two amorphous phases are defined besides the crystalline fraction (CRF): mobile amorphous fraction (MAF) and rigid amorphous fraction (RAF) (Wunderlich, 2003; Rastogi et al., 2004). MAF is the conventional amorphous part, the same as the amorphous phase of a two-phase morphological model. RAF is located on the boundary of crystalline parts and is composed of molecule chains that can be found both in the crystalline and the amorphous parts. The segments of these chains that are next to crystallites are hindered

in their movement, which can have a significant effect on mechanical properties (Badia et al., 2012; Androsch, 2008).

The aim of research was to investigate the mechanical properties of recycled PET samples as well as their change as a function of time. The properties were examined in the four weeks after production. This time interval is longer than that of usual aging experiments, but shorter than that of long-time behavior (creep, relaxation) experiments. Samples were injection moulded from recycled poly(ethylene-terephthalate) granulate. To understand the changes in mechanical properties, both the morphology of injection moulded samples and recycled granulates were investigated. Relationship between the morphological and mechanical properties of injection moulded products and their change as a function of time elapsed since production was also examined. Deeper understanding of the change of mechanical properties and their correlation with the morphology as a function of time elapsed after production can help us to produce higher quality products from recycled PET.

2. Experimental

2.1 Materials

NeoPET 80 (Neo Group, Lithuania) granulates the intrinsic viscosity (IV) of which was 0.8 dl/g were used in the experiments. To model the recycled material regranulates were extruded without drying from the original material, and this way a shorter molecule chain, degraded material was obtained (hereinafter referred to as RPET), the IV value of which was 0.61 ± 0.01 dl/g. Compared to the commercial recycled material (flakes or pellets) these regranulates are free of contamination, and the IV values are in the same range. To explain the morphology of injection moulded products regranulates with IV value 0.52 ± 0.01 dl/g were also manufactured

(by extrusion two times) besides RPET, the IV of which was nearly equal to the IV of the injection moulded samples (0.54 ± 0.01 dl/g).

2.2 Injection Moulding and Sample Preparation

Regranulates were dried in a Heraeus UT20 air circulation drying oven at 160 °C for 6 hours before injection moulding. 80 mm x 80 mm x 2 mm plaque mouldings were injection moulded in an Arburg Allrounder Advance 370S 700-290 machine. Melt temperature was 280 °C, mould temperature was 60 °C, and injection rate was 45 cm³/s. The specimens were cut to 10 mm wide slices parallel to the flow direction for morphological and mechanical examinations.

2.3 Characterization

The intrinsic viscosity of the base material and the specimens was determined using a computer controlled PSL Rheotek automatic solution viscometer equipped with optical sensor. Phenol-tetrachloroethane mixture in the ratio of 60:40% was applied as solvent, concentration was 0.5 g/dl, and examination temperature was 30 °C. The morphological characteristics of RPET reggranulates and injection moulded specimens were determined with a DSC device type Setaram DSC131 EVO. One heating phase was applied during the measurement between 20 and 290 °C, at 10 °C/min heating rate. The weight of examined samples was between 6 and 8 mg. The material structures were characterized with the three-phase model during the examinations. Crystalline fraction (CRF) was calculated using equation (1):

$$CRF = \frac{\Delta h_m - \sum \Delta h_{cc}}{\Delta h_m^0} 100\% , \quad (1)$$

where CRF is crystalline fraction in the sample [%], Δh_m is the specific heat of melting referenced to sample mass [J/g], Δh_{cc} is the specific heat of cold crystallization referenced to sample mass [J/g], Δh_m^0 is the heat of fusion of 100% crystalline PET (140.1 J/g) (Badia et al.,

2012). The amount of mobile amorphous fraction (MAF) was determined based on the specific heat change measured during glass transition using equation (2):

$$MAF = \frac{\Delta c_p}{\Delta c_p^0} 100\% , \quad (2)$$

where *MAF* is mobile amorphous fraction in the sample [%], Δc_p is the specific heat change measured during glass transition [$J/(g^\circ C)$], Δc_p^0 is the specific heat change of totally amorphous PET measured during glass transition ($0.405 J/(g^\circ C)$) (Badia et al., 2012). Rigid amorphous fraction (RAF) was determined using equation (3):

$$RAF = 100\% - MAF - CRF , \quad (3)$$

where *RAF* is rigid amorphous fraction in the sample [%], *MAF* is mobile amorphous fraction in the sample [%], *CRF* is crystalline fraction in the sample [%]. DSC examinations were carried out on slices cut from the skin and core part of injection moulded specimens. Slices were cut using cutting machine Leica RM 2125RT. When skin was examined, the slices were cut from the edge – 0.05 mm from the edge – of the specimen cross section, in case of the core, the middle 0.05 mm was used in the specimen cross section. Strength and modulus were determined on an Instron 3369 universal machine. Tensile modulus of elasticity was determined between 0.05% and 0.25% relative elongation at 1 mm/min crosshead speed, using a video extensometer. Tensile strength was determined at 10 mm/min crosshead speed. 5 specimens were tested in case of all measurements. Impact strength was determined by Izod impact tests on notched specimens using a 2.75 J hammer, at room temperature. 10 specimens were tested in case of all measurements. Morphological and mechanical properties of granulates and specimens were examined in the four weeks after production. The samples were stored in vacuum cabinet at 25 °C under vacuum after production.

3. Results and Discussion

3.2 Morphology of Granulates

DSC examinations were carried out in order to track the morphology change of one time and two times extruded granulates. Figure 1 shows the change of crystalline, rigid amorphous and mobile amorphous fractions of once extruded granulates in the examined period. Crystalline fraction fluctuated around 6%, RAF values deviated around 27%, MAF values fluctuated around 67% in the four weeks after manufacturing.

Figure 2 shows the change of CRF, RAF and MAF of two times extruded granulates in the four weeks after manufacturing. Similarly to one time extruded samples, the CRF, RAF and MAF also fluctuated around a mean value that can be considered as a constant in case of all samples. CRF was always around 8%, RAF values deviated around 26%, MAF values deviated around 66%. Based on these results it can be stated that no morphological change took place after production in case of regranulates with different IV values.

3.2 Morphology of Injection Moulded Samples

After regranulates were examined, specimens were injection moulded from one time extruded RPET, both morphological and mechanical properties were investigated as a function of time elapsed since manufacturing. The IV of specimens after injection moulding was 0.54 ± 0.01 dl/g. Figure 3 shows the morphological properties and their change as a function of time elapsed since manufacturing of the core part of specimens.

Significant changes can be observed in the structure of the core part of the specimens in the four weeks after manufacturing. CRF increased from 6% to 10%, while RAF decreased by 14%, and MAF increased by 10%.

If the rigid amorphous fraction is assumed to be between the folding surfaces of the crystallites and the mobile amorphous regions (Androsch, 2008), the results refer to a post crystallization process that took place after manufacturing, i.e. rigid amorphous chain parts increased

crystalline size, and therefore crystalline fraction as well (Figure 4). Increase of crystalline size is confirmed by DSC curves. The offset temperature of melting peaks increased in the four weeks after manufacturing (Figure 5), and that refers to larger crystallites (Ehrenstein, 2004). During chain rearrangement process, secondary bonds may break (e. g. since chains approach a state of equilibrium), and parallel with this new bonds may form. If the amount of the broken secondary bonds is higher than that of the formed bonds in the interphase of the rigid and mobile amorphous fractions, it can increase the mobile amorphous fraction as well (Figure 6).

Figure 7 reveals the morphological properties of the skin part in specimens and their change as a function of time elapsed since manufacturing. CRF increased from 5% to 10%, RAF decreased by 6%, while MAF increased to a small extent, by 1%. RAF-CRF rearrangement (increase in crystallinity) can also be experienced here, however it is smaller than in case of the core part, and the change of mobile amorphous fraction was also not significant. The reason for this difference can be that the core part of samples was thicker than the skin part resulting in a slower cooling rate and longer crystallization time, hence initial crystallinity was larger and more perfect crystalline parts could form in the material, and that could hinder post crystallization process.

Morphological examination results of granulates and specimens reveal that post crystallization of samples is not related to the structure of the base material since crystalline fraction of granulates with different IV did not change in the four weeks after manufacturing. The reason for the significant increase in case of injection moulded samples is the morphological structure formed during processing that is influenced by the technological parameters (such as shearing – orientation; temperatures, wall thickness, cooling time – crystallization) significantly.

3.3 Mechanical Properties

Mechanical properties also changed significantly in the four weeks after manufacturing besides morphological properties. In the four weeks after manufacturing, tensile strength increased from 49 MPa to 56 MPa, and modulus increased from 1860 MPa to 1990 MPa (Figure 8). Strength increase can be traced back to two phenomena. First of all, to crystalline fraction increase as a result of which several organized parts are formed, the mechanical properties of which are better than that of amorphous parts; another reason can be the structure change of amorphous parts, which can be similar to orientation effect. This structure change can be caused by the rearrangement of the amorphous segments due to the RAF-MAF (and indirectly due to the RAF-CRF) transformation, or the aging effect of the MAF. The modulus increase after production can be traced back to post crystallization, and within that MAF structure change can cause the experienced increase.

Figure 9 shows the impact strength change of specimens as a function of time. The impact strength of specimens decreased from 3.5 kJ/m² to 2.8 kJ/m² in the four weeks after manufacturing. There are more reasons for this decrease: one is the increase of crystalline fraction and the size of crystalline parts that result in larger crystallites with larger boundary surfaces and with smaller distance among them, and this way crack propagation path may decrease.

4. Conclusions

Change of mechanical properties after manufacturing in case of products made of recycled PET cannot be determined unambiguously in advance. In order to be able to manufacture adequate products these properties have to be known as precisely as possible. During research, both morphological and mechanical properties of regranulates with different IV values and injection moulded specimens and their change as a function of time elapsed since manufacturing were examined.

In case of injection moulded products a significant crystalline fraction increase was experienced in the four weeks after manufacturing both in the core and skin parts of the sample. In case of regranulates, this was not the case, therefore post crystallization of injection moulded specimens is not traced back to the IV value of the base material but to the processing parameters (such as shears, cooling rates), i.e. material structural properties (such as core-skin structure, orientation) formed during production.

During post crystallization the rigid amorphous fraction of samples decreased, the quantity of mobile amorphous phase increased both in the core and skin parts. The rigid amorphous fraction increased the size of crystalline parts. Through molecule chain rearrangement secondary bonds broke, and new bonds were also formed and mobile amorphous fraction increased in the core part of the samples. During this process not only crystallinity but also the structure of mobile amorphous parts could change.

Morphology results are also reflected in the change of mechanical properties. The tensile strength and tensile modulus of elasticity of injection moulded samples increased in the four weeks after production. This can be explained by the increase of crystallinity and the orientation of the mobile amorphous fraction. Impact strength decreased significantly after manufacturing and that is related to the increase in the size of crystalline parts (shorter crack propagation path) and to the change of the mobile amorphous structure in the samples (smaller mobility, smaller energy absorbing capability).

Based on the results it can be concluded that significant changes of mechanical and morphological properties of recycled PET are caused by technological parameters, not by the IV value of regranulates. Understanding changes of mechanical properties of injection moulded samples and finding the correlation with morphology, and their change as a function of time elapsed after production can help us to control the properties of injection moulded samples.

Acknowledgements

The infrastructure of the research project was supported by the Hungarian Scientific Research Fund (OTKA K109224).

References

- Alvarez, C., Sics, I., Nogales, A., Denchev, Z., Funari, S. S., Ezquerra, T. A., “Structure-dynamic relationship in crystallizing poly(ethylene terephthalate) as revealed by time-resolved X-Ray dielectric methods”, *Polymer*, 45, 3953-3959 (2004), DOI:10.1016/j.polymer.2003.09.069
- Androsch, R., “Surface structure of folded-chain crystals of poly(R-3-hydroxybutyrate) of different chain length”, *Polymer*, 49, 4673-4679 (2008), DOI:10.1016/j.polymer.2008.08.26
- Assadi, R., Colin, X., Verdu, J., “Irreversible structural changes during PET recycling by extrusion”, *Polymer*, 45, 4403-4412 (2004), DOI:10.1016/j.polymer.2004.04.029
- Badia, J. D., Strömberg, E., Karlsson, S., Ribes-Greus, A., “The role of crystalline, mobile amorphous rigid amorphous fractions in the performance of recycled poly (ethylene terephthalate) (PET)”, *Polym. Degrad. Stabil.*, 97, 98-107 (2012), DOI:10.1016/j.polymdegradstab.2011.10.008
- Choi, Y. W., Moon, D. J., Kim, Y. J., Lachemi, M., “Characteristic of mortar and concrete containing fine aggregate manufactured from recycled waste polyethylene terephthalate bottles”, *Constr. Build. Mater.*, 23, 2829-2835 (2009), DOI:10.1016/j.conbuildmat.2009.02.036
- Dobrovsky, K., Ronkay, F., “Effects of SEBS-g-MA on rheology, morphology and mechanical properties of PET/HDPE blends”, *Int. Polym. Proc.*, 30, 91-99 (2015), DOI:10.3139/217.2970
- Ehrenstein, G. W., Riedel, G., Trawiel, P.: *Thermal Analysis of Plastics*, 1st edition, Hanser Publishers, Munich, (2004), DOI:10.3139/9783446434141

- Ge, Z., Huang, D., Sun, R., Gao, Z., “Properties of plastic mortar made with recycled polyethylene terephthalate”, *Constr. Build. Mater.*, 73, 682-687 (2014), DOI:10.1016/j.conbuildmat.2014.10.005
- Gowd, E. B., Ramesh, C., Byrne, M. S., Murthy, N. S., Radhakrishnan, J., “Effect of molecular orientation on the crystallization and melting behavior in poly(ethylene terephthalate)”, *Polymer*, 45, 6707-6712 (2004), DOI:10.1016/j.polymer.2004.07.025
- Hamonic, F., Miri, V., Saiter, A., Dargent, E., “Rigid amorphous fraction versus oriented amorphous fraction in uniaxially drawn polyesters”, *Eur. Polym. J.*, 58, 233-244 (2014), DOI:10.1016/j.eurpolymj.2014.06.014
- Hao, W., Wang, X., Yang, W., Zheng, K., “Non-isothermal crystallization kinetics of recycled PET-Si₃N₄ nanocomposites”, *Polym. Test.*, 31, 110-116 (2012), DOI:10.1016/j.polymertesting.2011.10.003
- Hsiao, B. S. et al., “Chapter 1 Experimental techniques”, in *Handbook of Polymer Crystallization*, Piorkowska, L. and Rutledge, G. C. (Ed.), John Wiley & Sons Inc., New Jersey, p. 1-30 (2013), DOI: 10.1002/9781118541838
- Incarinato, L., Scarfato, P., Maio, L. D., Acierno D., “Structure rheology of recycled PET modified by reactive extrusion”, *Polymer*, 41, 6825-6831 (2000), DOI:10.1016/S0032-3861(00)00032-X
- Karagiannidis, P. G., Stergiou, A. C., Karayannidis, G. P., “Study of crystallinity and thermomechanical analysis of annealed poly(ethylene terephthalate) films”, *Eur. Polym. J.*, 44, 1475-1486 (2008), DOI:10.1016/j.eurpolymj.2008.02.024
- Karayannidis, G. P., Psalida, E. A., “Chain Extension of Recycled Poly(ethylene terephthalate) with 2,2'-(1,4-phenylene)bis(2-oxazoline)”, *J. Appl. Polym. Sci.*, 77, 2206-2211 (2000), DOI: 10.1002/1097-4628(20000906)77:103.0.CO;2-D

- Lei, Y., Wu, Q., Zhang, Q., “Morphology and properties of microfibrillar composites based on recycled poly (ethylene terephthalate) and high density polyethylene”, *Compos. Part. A.-Appl. S.*, 40, 904-912 (2009), DOI:10.1016/j.compositesa.2009.04.017
- López, M. d. M. C., Pernas, A. I. A., López, M. J. A., Latorre, A. L., Vilarino, J. M. L., Rodríguez, M. V. G., “Assessing changes on poly(ethylene terephthalate) properties after recycling: Mechanical recycling in laboratory versus postconsumer recycled material”, *Mater. Chem. Phys.*, 147, 884-894 (2014), DOI:10.1016/j.matchemphys.2014.06.034
- Meri, R. M., Zicans, J., Maksimovs, R., Ivanova, T., Kalnins, M., Berzina, R., Japins, G., “Elasticity long-term behavior of recycled polyethylene terephthalate (rPET)/montmorillonite (MMT) composites”, *Compos. Struct.*, 111, 453-458 (2014), DOI:10.1016/j.compstruct.2014.01.017
- Moghaddam, T. B., Soltani, M., Karim, M. R., “Stiffness modulus of Polyethylene Terephthalate modified asphalt mixture: A statistical analysis of the laboratory testing results”, *Mater. Design.*, 68, 88-96 (2015), DOI:10.1016/j.matdes.2014.11.044
- Paci, M., Mantia, F. P. L., “Influence of small amounts of polyvinylchloride on the recycling of polyethyleneterephthalate”, *Polym. Degrad. Stabil.*, 63, 11-14 (1999), DOI:10.1016/S0141-3910(98)00053-6
- Pegoretti, A., Penati, A., “Recycled poly(ethylene terephthalate) and its short glass fibres composites: effect of hygrothermal aging on the thermo-mechanical behavior”, *Polymer*, 45, 7995-8004 (2004), DOI:10.1016/j.polymer.2004.09.034
- Raffa, P., Coltelli, M-B., Savi, S., Bianchi, S., Castelvetro, V., “Chain extension and branching of poly(ethylene terephthalate) (PET) with di- multifunctional epoxy or isocyanate additives: An experimental and modelling study”, *React. Funct. Polym.*, 72, 50-60 (2012), DOI:10.1016/j.reactfunctpolym.2011.10.007

- Rastogi, R., Vellinga, W. P., Rastogi, S., Schick, C., Meijer, H. E. H., “The Three-Phase Structure and Mechanical Properties of Poly(ethylene terephthalate)”, *J. Polym. Sci. Pol. Phys.*, 42, 2092-2106 (2004), DOI:10.1002/polb.20096
- Tao, Y., Mai, K., “Non-isothermal crystallization and melting behavior of compatibilized polypropylene/recycled poly(ethylene terephthalate) blends”, *Eur. Polym. J.*, 43, 3538-3549 (2007), DOI:10.1016/j.eurpolymj.2007.05.007
- Torres, N., Robin, J. J., Boutevin, B., “Study of thermal and mechanical properties of virgin and recycled poly(ethylene terephthalate) before after injection molding”, *Eur. Polym. J.*, 36, 2075-2080 (2000), DOI:10.1016/S0014-3057(99)00301-8
- Viana, J. C., Alves, N. M., Mano, J. F., “Morphology Mechanical Properties of Injection Molded Poly(Ethylene Terephthalate)”, *Polym. Eng. Sci.*, 44, 2174-2184 (2004), DOI:10.1002/pen.20245
- Welle, F., “Twenty years of PET bottle to bottle recycling – An overview”, *Resour. Conserv. Recy.*, 55, 865-875 (2011), DOI:10.1016/j.resconrec.2011.04.009
- Wunderlich, B., „Reversible crystallization and the rigid-amorphous phase in semicrystalline macromolecules”, *Prog. Polym. Sci.*, 28, 383-450 (2003), DOI:10.1016/S0079-6700(02)00085-0
- Zare, Y., “Recent progress on preparation and properties of nanocomposites from recycled polymers: A review”, *Waste Manage.*, 33, 598-604 (2013), DOI:10.1016/j.wasman.2012.07.031

Figure 1. Crystalline, mobile amorphous and rigid amorphous fractions of granulates with IV=0.61 dl/g as a function time elapsed since manufacturing

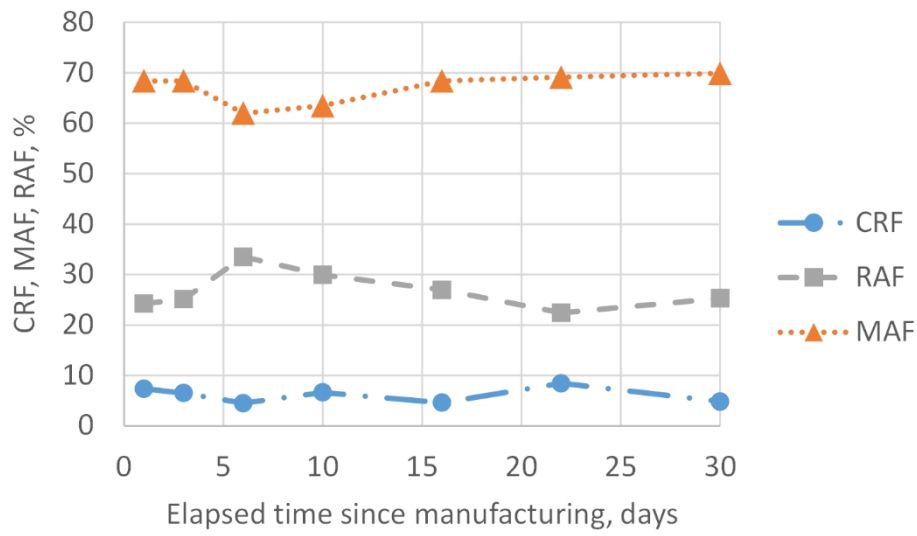


Figure 2. Crystalline, mobile amorphous and rigid amorphous fractions of granulates with IV= 0.52 dl/g as a function time elapsed since manufacturing

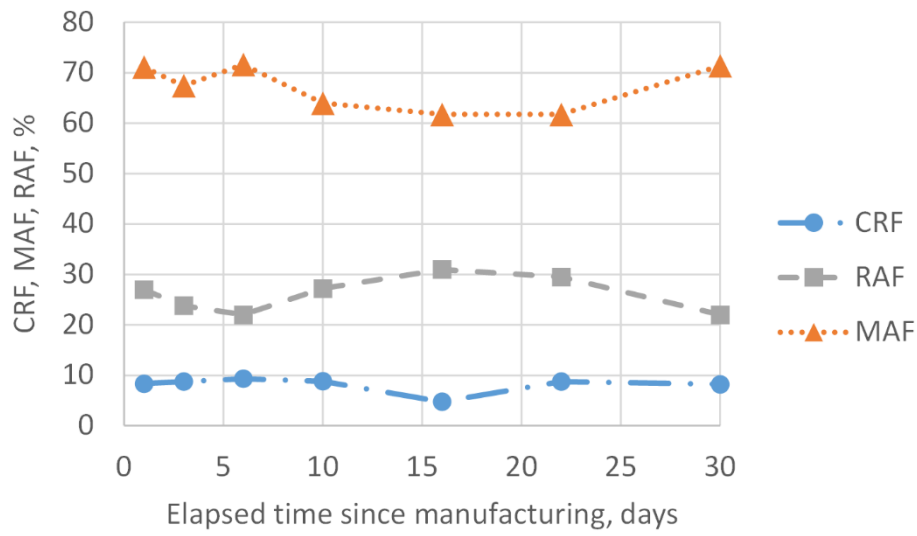


Figure 3. Morphology of core part in specimens as a function time elapsed since manufacturing

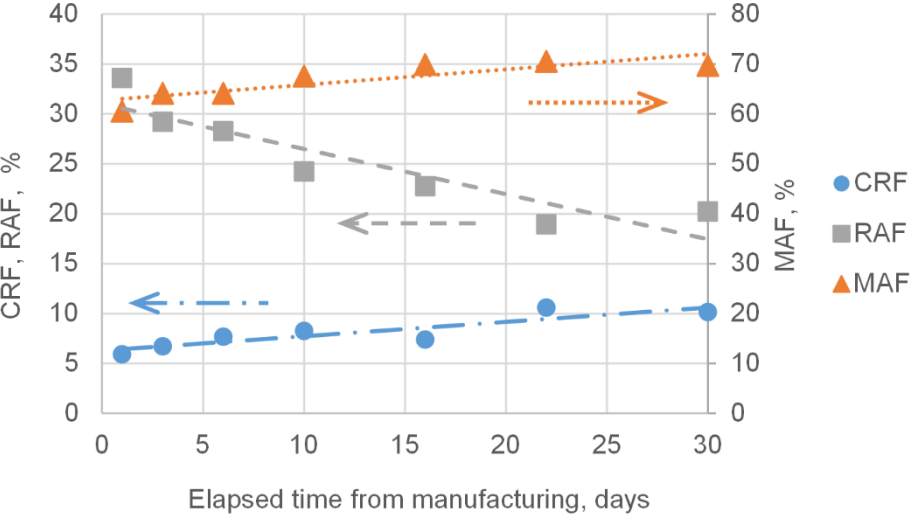


Figure 4. Process of post crystallization

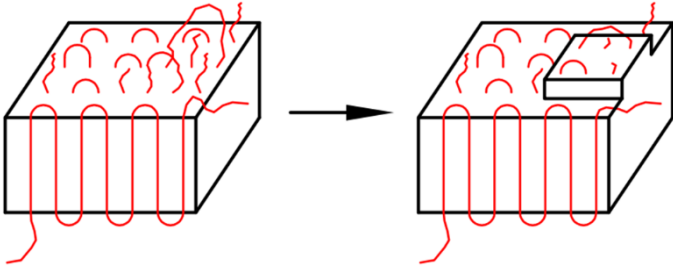


Figure 5. Offset point of DSC melting peaks as a function time elapsed since manufacturing

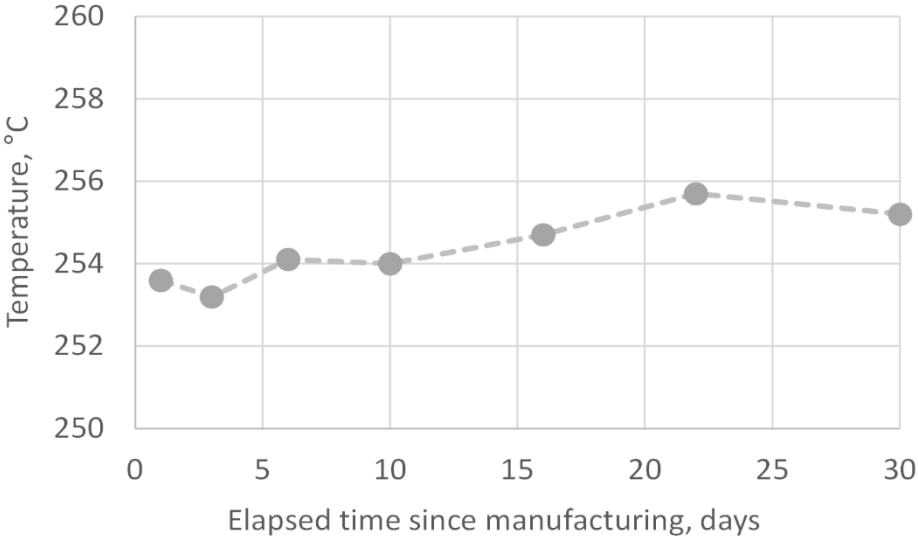


Figure 6. RAF-CRF and RAF-MAF rearrangement during the post-crystallization process

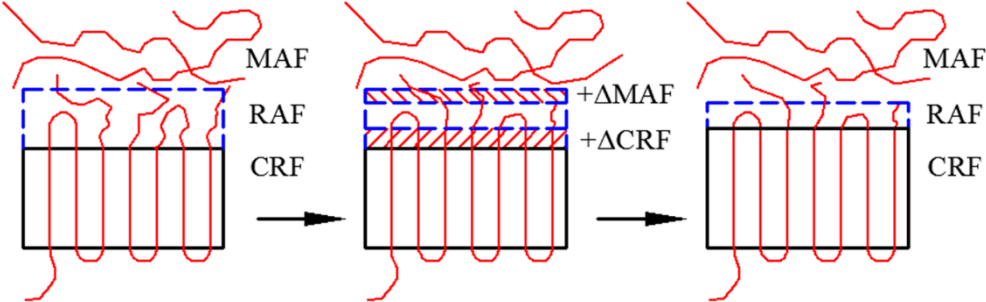


Figure 7. Morphology of skin part in specimens as a function time elapsed since manufacturing

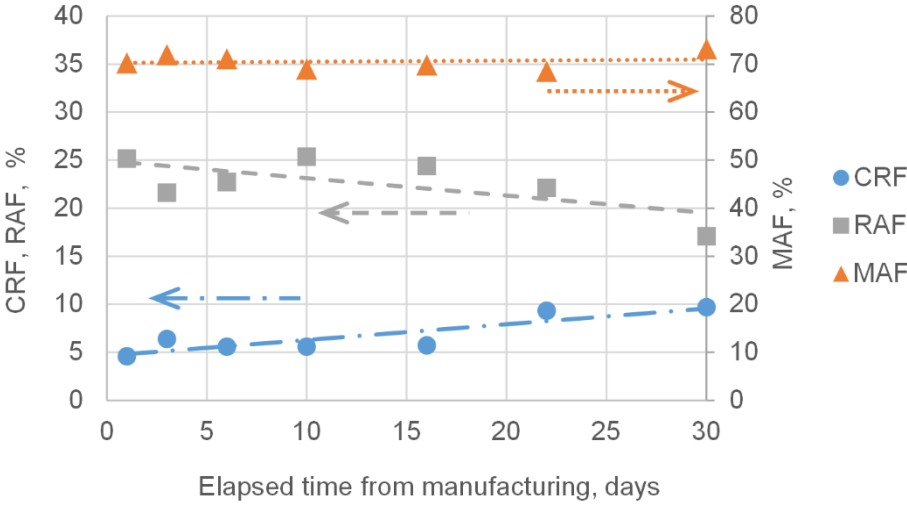


Figure 8. Tensile strength and modulus of specimens as a function time elapsed since manufacturing

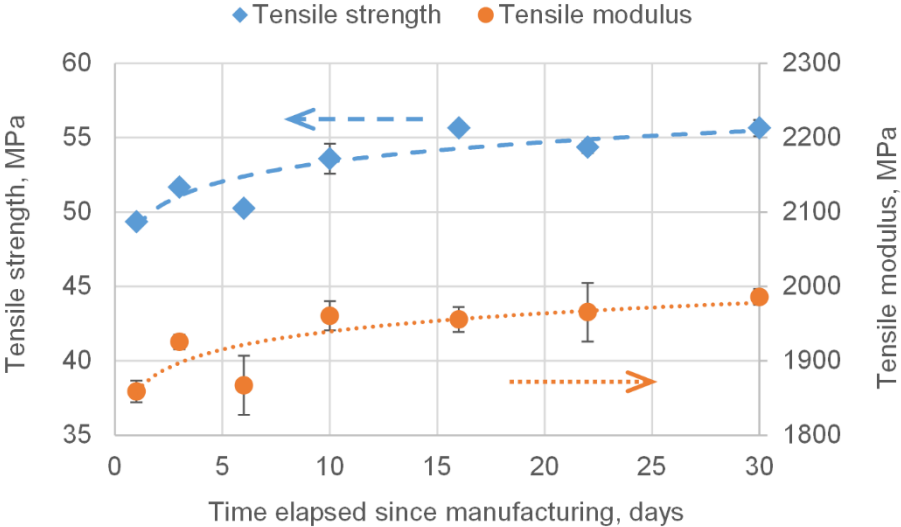


Figure 9. Impact strength (Izod, notched) of specimens as a function time elapsed since manufacturing

